An Image Catalogue of Micron- and Sub-micron- sized constrictions fabricated with the Femtosecond laser and created with the AFM.

Patrice Umenne[1*]

[1]Department of Electrical Engineering, University of South Africa; umennpo@unisa.ac.za
Correspondence: umennpo@unisa.ac.za; Tel: (+27 11-471-3482)

Abstract: In this paper a set of constrictions in the micron and sub-micron range fabricated with the femtosecond laser on superconducting $YBa_2Cu_3O_7$ thin film are scanned with the Atomic Force Microscope (AFM). The AFM images of the resulting constrictions are depicted. The width of the constrictions fabricated range from 1.24 µm micron dimension to 812 nm in the sub-micron range. The laser ablation spot size or diameter is set at 15.8 µm for the femtosecond laser and the separation distance between the centers of the laser ablation spots is varied between (16 – 17) µm as a result generating the variable constriction widths for the different superconductive bridges. The images of the fabricated micron and sub-micron constrictions are shown as a catalogue in the paper. The AFM images also show the surface morphology of the fabricated constriction qubits.

Keywords: Atomic Force Microscope (AFM) images; Constrictions; Femtosecond laser; Laser ablation spot size; Separation distance between the centers of the laser ablation spots.

1. Introduction

In this paper the femtosecond laser [1-4] was used to fabricate micron and sub-micron sized constrictions on the superconducting Yttrium barium copper oxide (YBCO) [5-7] thin films. These superconducting constrictions can be used as Josephson Junctions [8-12]. Other lasers [13-15] have been utilized to fabricate superconductive constrictions and Josephson Junctions. The main aim of utilizing the femtosecond laser to fabricate superconductive cubits is because of its low pulse duration. This specific femtosecond laser has a pulse duration [16-18] of $130 \times 10^{-15}\, s$. The low pulse duration of the femtosecond laser helps to reduce the thermal heating [19] or localized heating [20] of the superconductive thin film by the femtosecond laser. This is very important because superconductive materials are sensitive to high temperatures which cause thermal degradation of the thin film and can lower the critical temperature (T_C) of the superconductive thin film. The femtosecond laser system used to fabricate the constrictions consists of the translation stage feed-rate, the pulse repetition rate or frequency of the laser source and the natural pulse duration of the femtosecond laser. The resulting average pulse duration of the overall femtosecond laser system is higher than the pulse duration of the innate femtosecond laser itself. Hence some thermal heating of the thin film occurs. The catalogue of images for the micron and sub-micron constrictions fabricated is given as a list in this paper. This specific catalogue of constrictions has never been depicted before. This paper consists of section 1 which introduces the paper, section 2 which briefly describes the method used, section 3, which gives the results including the AFM images and discusses the paper and Section 4 which concludes the paper.

2. Materials and Methods

2.1. Femtosecond laser setup

The Femtosecond laser that was used to machine the micron- and sub-micron- sized constrictions has a pulse duration of $130 \times 10^{-15}\,s$ and a wavelength of 775 nm. The power output range of the femtosecond laser is (0-1000) mW, but to fabricate the constrictions, it was set at 2.1 mW. This power output level helps to make the laser ablation spot size smaller and hence achieve constrictions on the micron and sub-micron scale. The frequency or pulse repetition rate of the laser was set at 1 kHz. The feed rate of the translation stage which holds the YBCO thin film during machining of the sample was configured to 20 mm/min or 333 μms^{-1}. The achieved laser ablation spot size using these settings was 15.8 μm. The separation distance between the centers of the laser ablation spots was varied in the range (16 – 17) µm using G-code software to control the movement of the translation stage. Thus, achieving constrictions whose widths range from 1.248 μm in the micron range to 812.4 nm in the sub-micron range. The width of these constrictions is given by the formula in equation (1) sourced from [1,2].

$$width\ of\ the\ constrictions\ (w) = separation\ distance\ between\ the\ centres\ of\ the\ laser\ ablations\ spots\ (S_W) - laser\ ablation\ spot\ size \quad (1)$$

Where w is the width of the constriction and S_W is the separation distance between the centers of the laser ablation spots. The schematic depicting these parameters on the fabricated constrictions is shown in Figure 1 below.

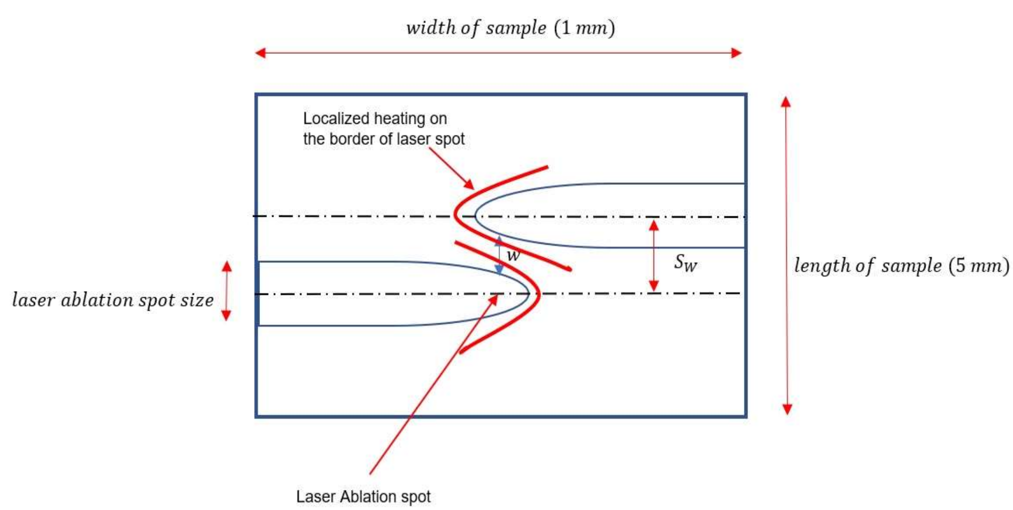

Figure 1. Schematic diagram of the shape of the fabricated constrictions and local heating [1]

2.2. YBCO Material used.

The YBCO thin films used to fabricate the constrictions were purchased from Ceraco GmBH and have a dimension of $(10\ \times 10\ \times 0.5)\ mm$. The YBCO thin films where fabricated using thermal reactive coevaporation method. The stoichiometric characteristics of the YBCO used are critical temperature $T_C = 86\ K$, the critical current density is $j_c(77\ K) \geq 2.0\ MA/cm^2$. The thin films are polished with YBCO on a single side with the thickness of YBCO being $0.2\ \mu m$ the rest is substrate material with a thickness of $499.8\ \mu m$. The substrates used where MgO and LAO. The constrictions space in Figure 1 above has a dimension of $(1 \times 5 \times 0.5)\ mm$. This means that up to 12 such constrictions were fabricated in each YBCO thin film with the femtosecond laser, that is 6 on the lower row and 6 on the upper row of the thin film.

2.3. Atomic Force Microscope (AFM) Model used.

The Atomic Force Microscope (AFM) [22] model "Nanosurf Flex FM 2011", shown in Figure 2 was used to scan the surface of the fabricated constrictions and derive the topographical images of the samples.

Figure 2. Atomic Force Microscope (AFM) "Nanosurf FlexAFM" [21]

The topographical images of the constrictions were created using the tapping mode of operation of the AFM in which the cantilever tip of the AFM is moved over the sample surface from left to right and back repeatedly. The cantilever tip scans transversely over the constriction space and across the laser ablation spots as can be seen in Figure 3, tapping the sample surface and generating the resultant image of the constrictions. The non-contact tapping mode is used because it does not damage the surface of the YBCO thin film.

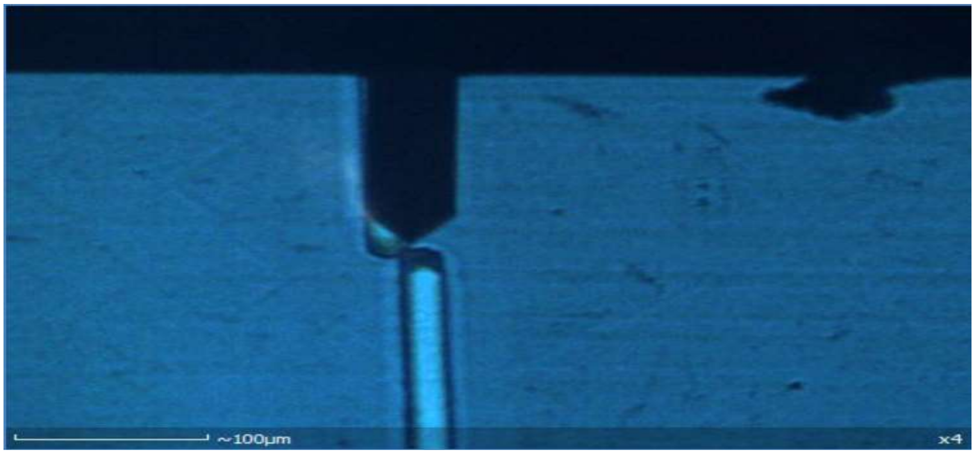

Figure 3. Cantilever tip of the AFM scanning the constriction space [21]

2.4. Overall Femtosecond Laser Setup for fabricating the constrictions.

The overall femtosecond laser setup for fabricating the constrictions is made up of the laser source (pump laser diode), the beam collimation setup which blows up the laser beam and then collimates it, the reflective mirrors, the iris or manual aperture for reducing the laser ablation spots size, the 30 mm spherical convex lens and the translation stage which holds the YBCO thin film for machining the constrictions. This setup can be seen in Figure 4. The iris or manual aperture diameter is reduced to $1500\ \mu m$ to enable just the centre core of the laser beam to continue to the focusing optics. The 30 mm spherical lens produces a laser ablation spot size of $15.8\ \mu m$. The translation stage is connected via a serial interface to a computer which runs the program for machining the constrictions. The program for machining the constrictions is written in the G-code programming language. The power level that is incident on the sample is approximately $2.1\ mW$.

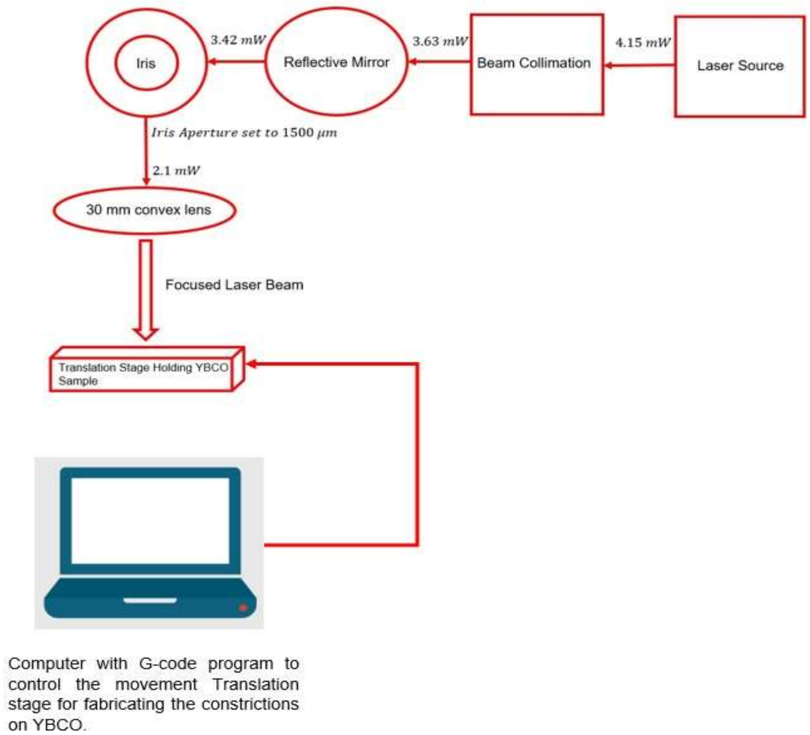

Figure 4. Overall block diagram depicting the Femtosecond Laser setup used to fabricate the constrictions [21]

3. Results

Table 1 below gives the list of constrictions fabricated with the femtosecond laser and scanned with the AFM. The table gives the constrictions from Micron-YBCO I to SubMicron YBCO VI. The laser ablation spot size is set at $15.8\ \mu m$. The separation distance between the laser ablation spots (S_W) is varied between $(17-16)$ µm in G-code programming. The power is specifically set to 2.035 mW. As a result, the constrictions widths fabricated vary from $1.24\ \mu m$ (micron) to $812\ nm$ (sub-micron) dimension following the formula in equation (1) sourced from [1,2] which was applied in the G-code program to move the translation stage.

Table 1. Catalogue of Constrictions fabricated on YBCO and their Specifications.

Number	Name of Constriction	Separation distance between the centers of the laser ablation spots (S_W)	Laser Ablation Spot Size	Width of Constriction	Power Setting
1	Micron-YBCO I	17 μm	15.8 μm	1.24 μm	2.035 mW
2	Micron-YBCO II	17 μm	15.8 μm	1.19 μm	2.035 mW
3	Micron-YBCO III	17 μm	15.8 μm	1.07 μm	2.035 mW
4	SubMicron-YBCO IV	16.5 μm	15.8 μm	879 nm	2.035 mW
5	SubMicron-YBCO V	16.5 μm	15.8 μm	874 nm	2.035 mW
6	SubMicron-YBCO VI	16 μm	15.8 μm	812 nm	2.035 mW

3.1. AFM imaging of Micron-YBCO I

Micron-YBCO I constriction fabricated with the femtosecond laser and scanned with the AFM can be seen in Figure 5 below. To fabricate the Micron-YBCO I constriction, the separation distance between the centers of the laser ablation spots was set a 17 μm, the laser ablation spot was 15.8 μm and the power configured to 2.035 mW. Using the AFM to scan the constriction gives the topographical line fit in Figure 5(a) which shows the width of the constriction to be 1.24 μm. Figure 5(b) is an amplitude line fit which shows the surface morphology of the constriction. Figure 5(c) gives the 3-D image of the constriction. The topographical line fit in Figure 5(a) gives the width of the constriction by measuring the width of the amplitude over the zero axis at the narrowest point of the constriction, since this is a variable width constriction. Judging from the 3-D imaging and the topographical line fit one can see that there is some thermal heating or localized heating of the YBCO sample by the femtosecond laser. The localized heating is evidenced by the darker shades or tinges in the AFM images on the border of the laser ablation spot. This effect is also portrayed in Figure 1 above. To get the image of this constriction the scan area was set to (19×19) μm.

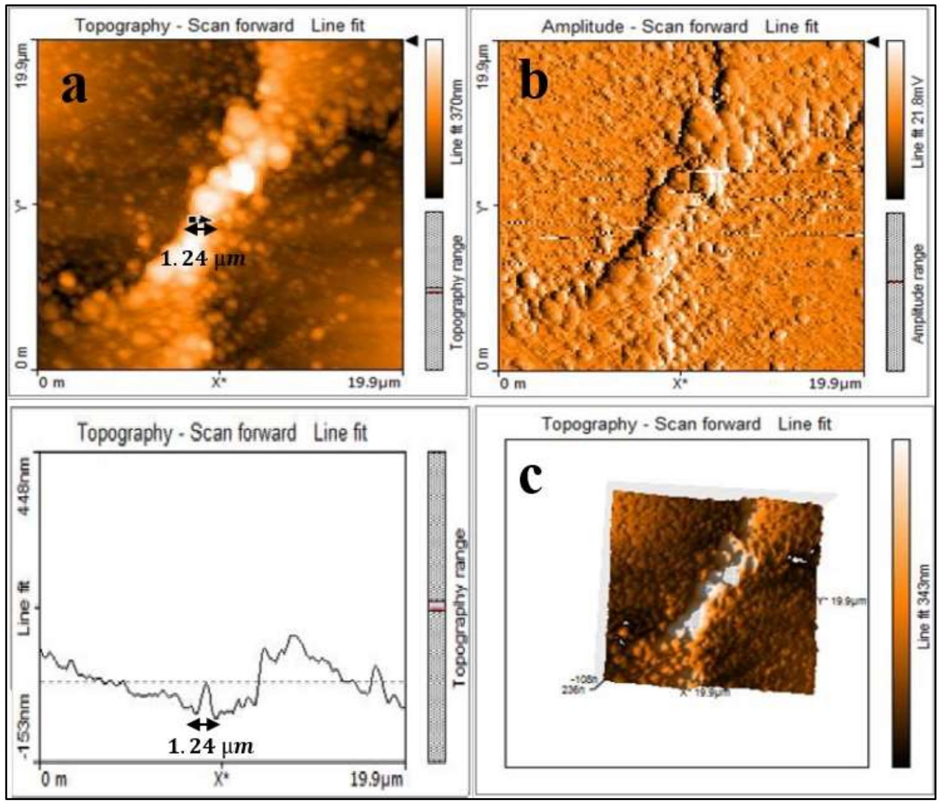

Figure 5. (a) Topography line fit of Micron-YBCO I shows the width of the Constriction to be 1.24 μm **(b)** Amplitude line fit of Micron-YBCO I showing outline **(c)** 3-D AFM plot of Micron-YBCO I

3.2 AFM imaging of Micron-YBCO II

Micron-YBCO II constriction fabricated with the femtosecond laser and scanned with the AFM can be seen in Figure 6 below. The S_W for the constriction was set at 17 μm, the laser ablation spot size is 15.8 μm and the power was set at 2.035 mW. The topographical line fit in Figure 6(a) shows the width of the constriction is 1.19 μm. Figure 6(b) is the amplitude line fit which shows the surface smoothness of the constriction, it can also be used to show the continuity of the constriction for conductive purposes. This constriction is continuous. Figure 6(c) gives the 3-D shape of the constriction. The topographical line fit in Figure 6(a) measures the width of the constriction by measuring the width of the amplitude over and above the zero axis at the narrowest point of the constriction. The scan area for this constriction was set at (20.5×20.5) μm.

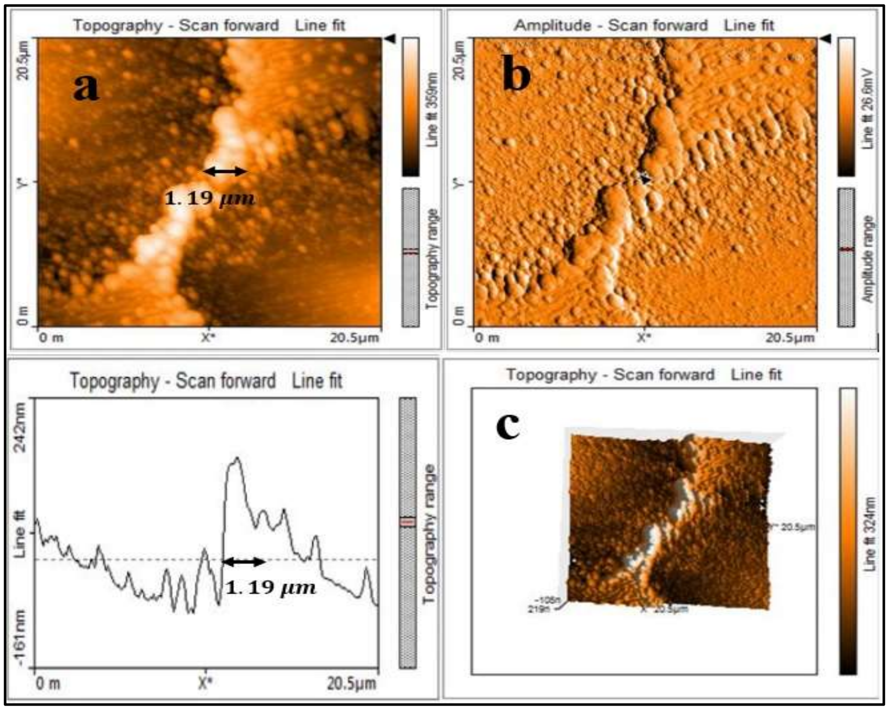

Figure 6. (a) Topography line fit of Micron-YBCO II shows the width of the Constriction to be 1.19 μm **(b)** Amplitude line fit of Micron-YBCO II showing outline **(c)** 3-D AFM plot of Micron-YBCO II

3.3 AFM imaging of Micron-YBCO III

During the fabrication of Micron-YBCO III Constriction the S_W is set to 17 μm, the laser ablation spot size is 15.8 μm and the laser power is configured to 2.035 mW. The topographical line fit in Figure 7(a) gives the width of the constriction as 1.07 μm. Figure 7(b) is the amplitude line fit of the constriction and Figure 7(c) the 3-D image of the constriction. The scan area for this constriction was set at (21.1×21.1) μm in the AFM.

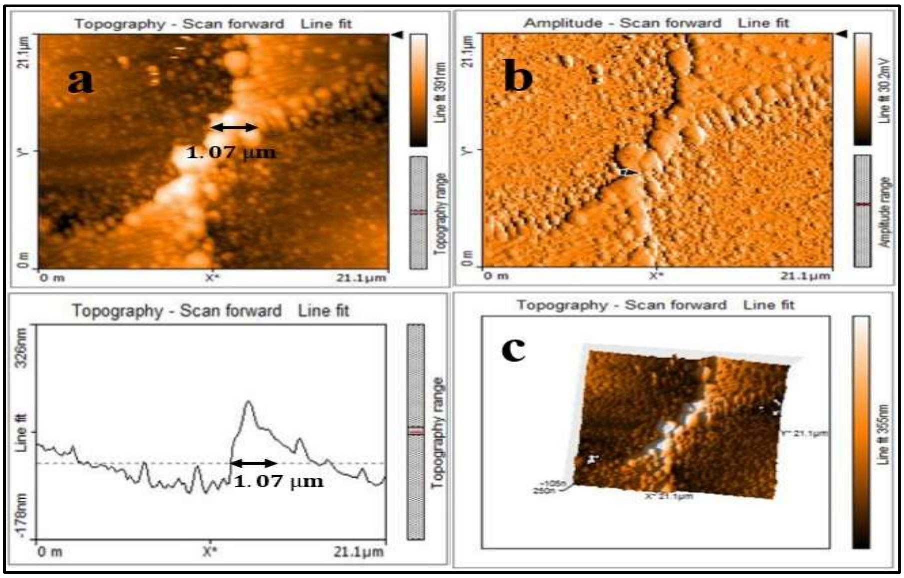

Figure 7. (a) Topography line fit of Micron-YBCO III shows the width of the Constriction to be 1.07 μm **(b)** Amplitude line fit of Micron-YBCO III showing outline **(c)** 3-D AFM plot of Micron-YBCO III

3.4 AFM imaging of SubMicron-YBCO IV

For SubMicron-YBCO IV constriction the S_W is 16.5 μm, the laser ablation spot size is also 15.8 μm and the laser power is 2.035 mW. The topographical line fit in Figure 8(a) indicates the width of the constriction is 879 nm. Figure 8(b) which shows the amplitude line fit indicates the constriction is continuous which is necessary for superconduction. Figure 8(c) gives the 3-D image of the constriction. The scan area used to derive the images was (17.6×17.6) μm.

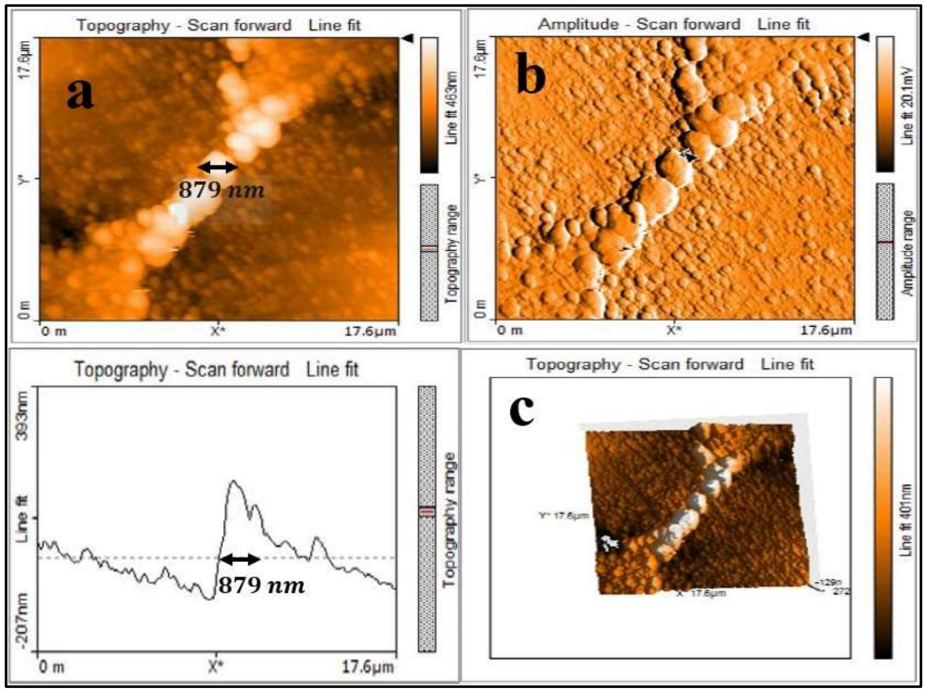

Figure 8. (a) Topography line fit of SubMicron-YBCO IV shows the width of the Constriction to be 879 nm **(b)** Amplitude line fit of SubMicron-YBCO IV showing outline **(c)** 3-D AFM plot of SubMicron-YBCO IV

3.5 AFM imaging of SubMicron-YBCO V

During the fabrication of SubMicron-YBCO V the S_W is reduced to 16.5 μm in the G-code. The laser ablation spot size is kept constant at 15.8 μm. The laser power is 2.035 mW. Following equation (1), source [1,2] the width of the constriction as given in the topographical line fit in Figure 9(a) reduces to 874 nm. The amplitude line fit in Figure 9(b) shows the constriction is not continuous. This is because the diffraction limit of the femtosecond laser whose wavelength is 775 nm is being approached. At this point it becomes quite difficult to make a continuous constriction without clipping the borders of the constriction with the laser. In order to achieve this specific optics such, as the planoconvex lens will be needed. The 3-D image in Figure 9(c) validates the constriction is not continuous. The scan area used to image the constriction is (19.6×19.6) μm.

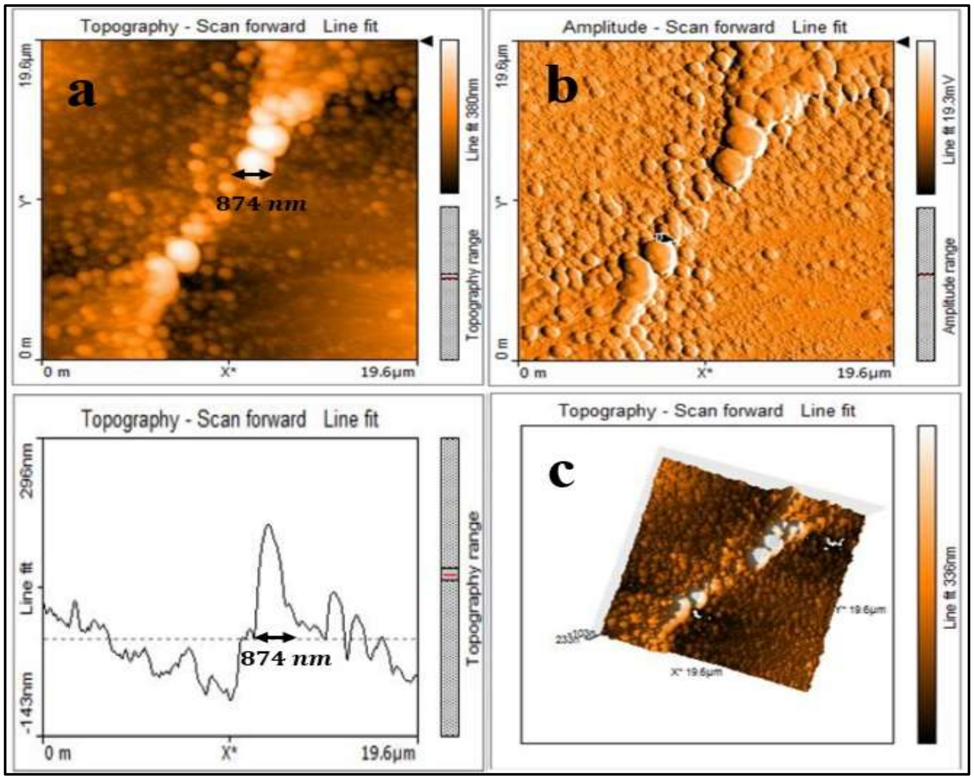

Figure 9. (a) Topography line fit of SubMicron-YBCO V shows the width of the Constriction to be 874 nm **(b)** Amplitude line fit of SubMicron-YBCO V showing outline **(c)** 3-D AFM plot of SubMicron-YBCO V

3.6 AFM imaging of SubMicron-YBCO VI

The S_W for SubMicron-YBCO VI Constriction is further reduced to 16 μm in the G-code. The laser ablation spot size is kept at 15.8 μm. The laser power is 2.035 mW. As a result, the width of the constriction reduces to 812 nm as indicated in the topographical line fit in Figure 10(a). Figure 10(b) shows the amplitude line fit which shows the constriction is continuous. The 3-D image of the constriction is given in Figure 10(c). The scan area of the constriction is set at (22.6×22.6) μm.

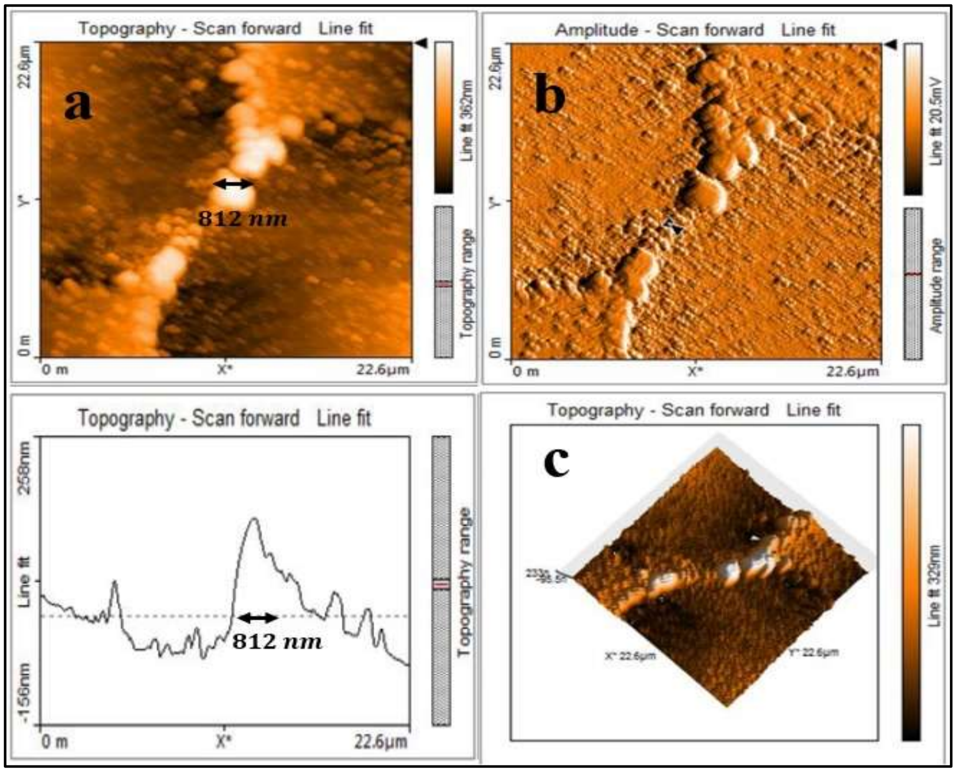

Figure 10. (a) Topography line fit of SubMicron-YBCO VI shows the width of the Constriction to be $812\ nm$ **(b)** Amplitude line fit of SubMicron-YBCO VI showing outline **(c)** 3-D AFM plot of SubMicron-YBCO VI

4. Discussion and Conclusion

In this paper a catalogue of constrictions machined using the femtosecond laser on the superconducting YBCO thin film are depicted and portrayed using the Atomic Force Microscope (AFM). The femtosecond laser has a very low pulse duration and can reduce the localized heating on the resultant constrictions. Due to the fact that in the femtosecond laser setup other components exist such as the translation stage and the laser source with a specific pulse frequency, the average time the laser spends on the YBCO thin film is much longer than femtoseconds and some thermal degradation occurs. This is evidenced by the darker shades on the YBCO thin film next to the laser spot in the AFM images. When the constrictions are being fabricated the separation distance between the laser ablation spots is reduced in the G-code program while the laser ablation spots size is kept constant. As a result, the widths of the fabricated constrictions reduced in size towards the nanoscale, which is validated by equation (1) [1,2]. This gives an element of control when fabricating nanoscale structures. The unique catalogue of images created by the AFM can assist to determine the physical continuity of fabricated constrictions in the micron, submicron, and nano scale.

Author Contributions: For research articles with several authors, a short paragraph specifying their individual contributions must be provided. The following statements should be used "Conceptualization, P.U methodology, P.U.; software, P.U.; validation, P.U.; formal analysis, P.U.; investigation, P.U.;

resources, P.U.; data curation, P.U.; writing—original draft preparation, P.U.; writing—review and editing, P.U.; visualization, P.U.; supervision, P.U.; project administration, P.U.; funding acquisition, P.U.; All authors have read and agreed to the published version of the manuscript."

Funding: This research was funded by University of South Africa, and The APC was funded by University of South Africa.

Institutional Review Board Statement: The study was conducted in accordance with the Declaration of Helsinki and approved by the Institutional Review Board (or Ethics Committee) of the UNIVERSITY OF SOUTH AFRICA for studies not involving humans or animals.

Informed Consent Statement: Not applicable.

Data Availability Statement: Data is unavailable.

Acknowledgments: I acknowledge the support provided by the University of South Africa.

Conflicts of Interest: Declare conflicts of interest or state "The author declares no conflict of interest."

References

1. Umenne, P.; Srinivasu, V.V. Femtosecond-laser fabrication of micron and sub-micron sized S-shaped constrictions on high T_C superconducting YBCO thin films: ablation and lithography issues. *J. Mater. Sci. Mater. Electron.* **2017**, vol. 28, issue no. 8, pp. 5817–5826, Available online: https://link.springer.com/article/10.1007/s10854-016-6253-z.
2. Umenne, P. Fabrication of S-shaped Micron Sized Constrictions on FeC (steel) surface using Femtosecond Laser Ablation with Beam Shaping. *Int. J. Adv. Manuf. Technol.* **2021,** vol. 116, issue no. (9-10), pp. 3043-3050, Available Online: https://doi.org/10.1007/s00170-021-07638-7.
3. Nivas, J.J.; Amoruso, S. Generation of Supra-Wavelength Grooves in Femtosecond Laser Surface Structuring of Silicon. *Nanomaterials (Basel).* **2021** vol. 11, issue no. 1, Article no. 174, Available online: https://doi.org/10.3390/nano11010174.
4. Qin, Y.; Batjargal, O.; Cromey, B.; Kieu, K. All-fiber high-power 1700 nm femtosecond laser based on optical parametric chirped-pulse amplification. *Opt. Express*. **2020**, vol. 28, issue no. 2, pp. 2317-2325, Available online: https://doi.org/10.1364/OE.384185.
5. Koblishka, M.R.; Naik, S.P.K.; Koblishka-Veneva, A.; Murakami, M.; Gokhfeld, D.; Reddy, E.S.; Schmitz, G.J. Superconducting YBCO Foams as Trapped Field Magnets. *Mater.* **2019,** vol. 12, issue no. 6, Article no. 853, Available Online: **https://doi.org/10.3390/ma12060853**
6. Sibanda, D.; Oyinbo, S.T.; Jen, T.; Ibitoye, A.I. A Mini Review on Thin Film Superconductors. *Process.* **2022,** vol. 10, issue no. 6, Article no. 1184, Available Online**:** **https://doi.org/10.3390/pr10061184**
7. Shipulin, I.A.; Thomas, A.A; Holleis, S.; Eisterer, M.; Nielsch, K.; Huhne, R. Effect of Silver Doping on the Superconducting and Structural Properties of YBCO Films Grown by PLD on Different Templates. *Mater.* **2022**, vol. 15, Issue no. 15, Article no. 5354, Available Online: **https://doi.org/10.3390/ma15155354**

8. Hertzberg, J.B.; Zhang, E.J.; Rosenblatt, S. *et al.* Laser-annealing Josephson junctions for yielding scaled-up superconducting quantum processors. *npj Quantum Inf.* **2021**, vol. 7, Article no. 129, Available Online: https://doi.org/10.1038/s41534-021-00464-5
9. Tafuri, F. Introduction: the Josephson Effect and Its Role in Physics. *J Supercond Nov Magn.* **2021**, vol. 34, pp. 1581–1586, Available Online: https://doi.org/10.1007/s10948-020-05775-w
10. Causanilles, F.S.V.; Baskonus, H.M.; Guirao, J.L.G.; Bermúdez, G.R. Some Important Points of the Josephson Effect via Two Superconductors in Complex Bases. *Mathematics.* **2022**, vol. 10, issue no. 15, Article no. 2591, Available online: https://doi.org/10.3390/math10152591
11. Ai, L.; Zhang, E.; Yang, J. *et al.* Van der Waals ferromagnetic Josephson junctions. *Nat Commun.* **2021,** vol. 12, Article no. 6580, Available online: https://doi.org/10.1038/s41467-021-26946-w
12. Zubarev, A.; Cuzminschi, M. Chaotic behavior of a stack of intrinsic Josephson junctions at the transition to branching for overcritical currents. *Chin. J. Phys.* **2021**, vol. 71, pp. 634-642, Available online: https://doi.org/10.1016/j.cjph.2021.03.025
13. Ashida, M.; Minowa, Y.; Kumakura, M.; Takahashi, Y.; Matsushima, F.; Moriwaki, Y. Fabrication of superconducting micro particles by laser ablation in superfluid helium. *Conference on Lasers and Electro-Optics (CLEO)*, San Jose, California, USA, 14-19th May 2017, pp. 1-2, Available online: https://ieeexplore.ieee.org/document/8084192
14. Elenskiy, I.; Tollkühn, M.; Kajevic, D.; Martens, M.; Hampel B.; Schilling, M. Fabrication and Properties of Josephson Junction Cantilevers for Terahertz Applications. *IEEE Trans. Appl. Supercond.* **2019**, vol. 29, issue no. 5, pp. 1-5, Available online: https://doi.org/10.1109/TASC.2019.2900217.
15. Magrini, W.; Mironov, S.V.; Rochet, A.; Tamarat, P.; Buzdin, A.I.; Lounis B. In-situ creation and control of Josephson junctions with a laser beam. *Appl. Phys. Lett*. **2019**, vol. 114, issue no. 14, pp. 142601 1-4, Available online: https://doi.org/10.1063/1.5086663
16. Zhang, K.; Ivanov, D.S.; Ganeev, R.A.; Boltaev, G.S.; Krishnendu, P.S.; Singh, S.C.; Garcia, M.E.; Zavestovskaya, I.N.; Guo, C. Pulse Duration and Wavelength Effects of Laser Ablation on the Oxidation, Hydrolysis, and Aging of Aluminum Nanoparticles in Water. *Nanomaterials* **2019**, vol. 9, issue no. 5, Article no. 767, Available online: https://doi.org/10.3390/nano9050767
17. Lauer, B.; Jaggi, B.; Neuenschwander, B. Influence of the pulse duration onto the material removal rate and machining quality for different types of Steel. *Phys. Procedia* **2014,** vol. 56, pp. 963-972, Available online: https://doi.org/10.1016/j.phpro.2014.08.116
18. Shih, C.; Shugaev, M.V.; Wu, C.; Zhigilei, L.V. The effect of pulse duration on nanoparticle generation in pulsed laser ablation in liquids: insights from large-scale atomistic simulations. *Phys. Chem. Chem. Phys.* **2020**, vol. 22, pp. 7077-7099, Available online: https://doi.org/10.1039/D0CP00608D
19. Haberkorn, N.; Bengio, S.; Suárez, S.; Pérez, P. D.; Hofer, J. A.; Sirena, M. Effect of thermal annealing and irradiation damage on the superconducting critical temperature of nanocrystalline

γ-Mo2N thin films. *Mater. Lett.* **2019**, vol. 236, pp. 252-255, Available online: https://doi.org/10.1016/j.matlet.2018.10.094

20. Lange, K.; Sparkes, M.; Bulmer, J.; Feighan, J. P. F.; O'neill, W.; Haugan, T. J. Analysing Laser Machined YBCO Microbridges Using Raman Spectroscopy and Transport Measurements Aiming to Investigate Process Induced Degradation. *Lasers in Eng*. **2020**, vol. 46, pp. 285-294.
21. Umenne, P. Fabrication of Nano Josephson Junctions Using the Femtosecond Laser Technique on High Tc Superconducting YBCO Thin films. PhD Dissertation, *University of South Africa*, Florida, Johannesburg, South Africa, June 2018, Available Online: http://hdl.handle.net/10500/23646
22. Umenne, P. AFM Analysis of Micron and Sub-Micron Sized Bridges Fabricated Using the Femtosecond Laser on YBCO Thin Films. *Micromachines* **2020**, vol. *11*, Article no. 1088, Available online: https://doi.org/10.3390/mi11121088